Desalination and Water Treatment
www.deswater.com

doi: 10.5004/dwt.2017.20780

77 (2017) 247–255
May

Characterization of pine-sawdust pyrolytic char activated by phosphoric acid through microwave irradiation and adsorption property toward CDNB in batch mode

Yubin Jiao[a], Danlu Han[b], Yizhen Lu[a], Yanchan Rong[a], Liyan Fang[a], Yali Liu[a], Runping Han[a,*]

[a]*College of Chemistry and Molecular Engineering, Zhengzhou University, No 100 Kexue Road, Zhengzhou 450001, China, Tel. +86 371 67781757; Fax: +86 371 67781556; emails: rphan67@zzu.edu.cn (R. Han), 361116201@qq.com (Y. Jiao), 1363493238@qq.com (Y. Lu), 429052746@qq.com (Y. Rong), 867839030@qq.com (L. Fang), yali1986_2006@126.com (Y. Liu)*
[b]*College of Physics and Technology, Wuhan University, No 299 Bayi Road, Wuhan 430072, China, Tel. +86 371 67781757; Fax: +86 371 67781556; email: 2025054902@qq.com*

Received 29 November 2016; Accepted 30 March 2017

ABSTRACT

In this research, pine-sawdust pyrolytic char (PyC) was activated by phosphoric acid through microwave irradiation and activated PyC (APC) was obtained. The characterization of APC was presented, such as scanning electron microscope, pH_{pzc}, Brunauer–Emmett–Teller surface area, surface functional group, etc. Surface area of APC was 683 m^2 g^{-1} while average radius of pore was 1.5 nm. Then, APC was used as adsorbent to remove 4-chloro-2,5-dimethoxy nitrobenzene (CDNB) from aqueous solution in batch mode. Several experimental factors like initial pH, NaCl concentration, contact time, solution temperature were evaluated. Solution pH within 2–5 was in favor of adsorption and common salts had no effect on adsorption quantity. The adsorption capacity from experiment was up to 220.8 mg g^{-1} at 297 K. Langmuir model and Freundlich model were used to fit the adsorption equilibrium data and both can better predict the process. The kinetic process was better fitted by pseudo-second-order kinetic model and the process was controlled by film diffusion process. CDNB-loaded APC can be regenerated by 70% ethanol and adsorption capacity decreased after regeneration. It was concluded that APC be good adsorbent to remove CDNB from solution.

Keywords: Activated pyrolytic char; Adsorption; CDNB; Regeneration

1. Introduction

Nitrobenzene compounds are frequently used by chemical industry such as the raw material in the manufacture of dyes, rubbers, pesticides and herbicides, pharmaceutical preparation, etc. [1]. These compounds have great harmful effect for public health and environmental quality and the wastewater has brought a series of serious environmental problem due to its high toxicity and accumulation in the environment [2]. Among the different processes often adopted for elimination of refractory pollutants, adsorption seems to be a good choice in terms of cost and operation for removal of aniline and its derivatives [3]. Adsorption on commercial activated carbon may be an effective process for removal of refractory pollutants from wastewater, but it is too expensive and the regeneration of spent activated carbon is relatively difficult with loss of mass [3]. So attentions have been focused on the development of low cost adsorbent for the application of wastewater treatment and there were several reviews in this field [3,4]. So, some raw or natural agricultural by-product and

* Corresponding author.

carbonaceous materials based on this by-product as low-cost adsorbents have been tested to evaluate their efficiency in the removal of dyes and other pollutants [5,6]. However, direct use of the raw agricultural by-products have many disadvantages, one of them is the leaching of organic pollutants, which may cause second pollution, second is the low adsorption capacity. The problem could be avoided by carbonization of the raw materials or chemical modification. Activated carbons, obtained from agricultural by-products, have good adsorption capacity with respect to heavy metals, phenol and dyes [7]. So carbonaceous material prepared was utilized as adsorbent for wastewater treatment. The transformation of agricultural residues into carbon or other products would avoid some problems of disposal and management of these waste by-products.

Recently, biomass was used to produce bio-oil or bio-gas production from pyrolysis and this may lead to the formation of solid residue, bio-char. Pyrolytic bio-char (PyC) is different from that formed by partial combustion. In the process of biomass thermal conversion, attention is usually focused on the liquid or gas product [8]. But bio-char as by-product has received attention in recent years. It is available for this carbonaceous residue used as soil amendment except direct combustion for heat production [9]. PyC can be directly used or simply modified as adsorbents for removal of heavy metal ions and dyes [10–12]. For enhancement of its surface property, PyC can be activated by physical or chemical methods to obtain activated carbon. The advantages of chemical activation are low energy cost due to lower temperature of process and higher product yield [13]. Compared with conventional heating process, microwave heating has the additional advantages: interior heating, higher heating rates, greater control of the heating process, etc. So the time can be considerably reduced and energy consumption was less [14–17]. Microwave assisted heating and chemical activation has been presented to prepare activated carbon and $ZnCl_2$, KOH, K_2CO_3, $NH_4H_2PO_4$, etc. were selected as activated agents [18–20]. The obtained carbon materials were selected as adsorbent. Agricultural residues as precursors can be used to prepare activated carbon and references of [21–24] were relative reviews.

4-Chloro-2,5-dimethoxy nitrobenzene (CDNB; as intermediate of dyes and pharmaceuticals), available in refined chemical process, can be released to wastewater during preparation process. It was selected as target pollutant as it is very difficult to biodegrade (chloro- or nitro-aromatic ring is more refractory) in wastewater treatment. Adsorption of CDNB was seldom studied by carbon or other materials. In this study, the pine-sawdust pyrolytic char (PyC) was activated by phosphoric acid through microwave irradiation and activated PyC (APC) was obtained. The characterization of APC was presented such as X-ray diffraction (XRD), scanning electron microscope (SEM), pH_{pzc} and pore structural parameters. Furthermore, CDNB was selected as adsorbate to study adsorption property of APC. Moreover, the equilibrium and kinetic data of the adsorption process were then analyzed to study the adsorption property. Regeneration of CDNB-loaded APC was also performed.

2. Materials and methods

2.1. Preparation of APC

PyC was obtained from Research Institute of Environmental Sciences, Zhengzhou University. It was produced by slow pyrolysis of biomass in a fluidized reactor to obtain pyrolytic oil. It was air-dried for 1 d and was ground and sieved to a particle size (30–80 mesh). Pine sawdust was adopted as the feedstock for the pyrolysis process in a fluidized-bed reactor. River sand was selected as medium and 2 kg h^{-1} of biomass can be treated [25]. The pyrolytic temperature is up to 550°C and the time through the fluidized bed is 5 min to produce bio-oil and bio-gas. The yield of PyC is about 25% of sawdust. Then, it was sieved to produce particles of 100–120 mesh and washed to remove dirty substances. The preparation procedure was as follows: PyC was soaked in H_3PO_4 solution (1:1) with an impregnation ratio of 1/5 (W/V). The activation step was conducted in a glass reactor placed in a microwave oven with a frequency of 2.45 GHz. The microwave power was set as 380 W and 2 min of irradiation time was selected as the heating period based on preliminary experiments. The activated product was then washed with hot HCl solution (V/V 1/10) solution (353 K and 2 h), sodium bicarbonate (0.1 mol L^{-1}) and deionized water until the pH of the washing solution reached 6–7, dried at 105°C and APC obtained was stored. The yield of APC is 66.4% (average of four times).

2.2. Characterization of PyC and APC

SEM analysis was performed to study the textural structure of PyC and APC. The pore structures of two materials were characterized by nitrogen adsorption at 77 K with an accelerated surface area and porosimetry system (Micromeritics ASAP 2020), while surface functional groups of APC were detected by Fourier transform infrared (FTIR) spectroscope (FTIR-2000, PerkinElmer, USA) from the scanning range of 4,000–400 cm^{-1}.

The amphoteric character of material surface was assessed by the selective acid–base neutralization method. Boehm titration [26] was used to determine the amount of surface acidic and basic functional groups. Each sample (0.400 g) was accurately weighed and reacted with 10 mL of 0.05 mol L^{-1} HCl, NaOH, Na_2CO_3, $NaHCO_3$ solution in a closed flask and agitated for 48 h at room temperature, respectively. Back titration was carried out. The suspensions was then decanted, and the remaining HCl, NaOH, Na_2CO_3, $NaHCO_3$, solution was determined by titration with 0.05 mol L^{-1} NaOH or HCl solution, respectively.

The determination of pH_{pzc} was conducted by adjusting pH of 20 mL 0.01 mol L^{-1} NaCl solution to a value between 2 and 11. APC or PyC of 0.010 g were added and the final pH was measured after 10 h under agitation. The pH_{pzc} is the point where $pH_i - pH_f = 0$.

X-ray diffraction (XRD) analysis was carried out to identify any crystallographic structure in PyC and APC sample using a computer-controlled X-ray diffractometer (D/MAX-RA, Japan). Content of carbon, nitrogen and hydrogen was determined by element analysis (Flash EA 1112, Thermo Electron Corporation, USA) while content of phosphorus, calcium and potassium was obtained by X-ray fluorescence analysis (S4PIONEER, German).

2.3. Preparation of CDNB solution

Molecular formula of CDNB is $C_8H_8ClNO_4$ and its molecular weight is 217.61 g mol^{-1} (CAS No 6940-53-0). Its structure

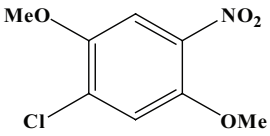

Fig. 1. Structure of CDNB.

is shown in Fig. 1. The CDNB used in this work was purchased from Luoyang Chemical Corporation, China. Solutions of CDNB were prepared to some desired concentration and pH of solution was near 6.2. The initial pH of the working solution was adjusted to the required value by addition of 1 mol L^{-1} HCl or NaOH solution before mixing with the adsorbents to study the effect of pH and the uptake pH was assumed constant during other experiments.

2.4. Adsorption study

Adsorption experiments were carried out in a rotary shaker at 100 rpm using 50 mL shaking flasks containing 20 mL of 30 mg L^{-1} CDNB concentrations with 0.004 g of APC. The experiments were carried out at 293, 303 and 313 K in a constant temperature shaker bath. After shaking the flasks for predetermined time intervals, the samples were withdrawn from the flask and then filtered with filter screen. The left out concentration in the supernatant solution was analyzed using a UV/Vis-3000 spectrophotometer at 281 nm. Each experiment was repeated three times and the results given were the average values. 450 min of contact time was selected to reach adsorption equilibrium except kinetic study.

The data obtained in batch studies were used to calculate CDNB uptake quantity. The quantity of dye loaded onto unit weight of APC (q_t or q_e, mg g^{-1}) was obtained using the following expression:

$$q = \frac{V(C_0 - C)}{m} \tag{1}$$

where C_0 is the initial CDNB concentration (mg L^{-1}), C is the CR concentration at any time t or equilibrium (mg L^{-1}), V is the CR solution volume (L) and m is the mass of APC (g).

To evaluate the reusability of APC, the regeneration and readsorption of CDNB studies were conducted for three consecutive cycles. Adsorption–desorption experiments were carried for the desorption solvent (20 mL 70% ethanol) to three cycles. A single cycle sequence consists of adsorption (300 min) followed by desorption (60 min) (pH = 3, APC dose = 0.2 g L^{-1}, C_0 = 30 mg L^{-1}, T = 303 K). After adsorption, the resultant CDNB-loaded APC was filtered, washed and air dried and reintroduced into the desorption solvent and agitated. The cycle of adsorption was performed. The desorption efficiency and regeneration efficiency were calculated in the following equations:

$$\rho = \frac{C_e \times V}{q_e \times m} \times 100\% \tag{2}$$

$$\eta = \frac{q_i}{q_b} \times 100\% \tag{3}$$

where ρ is desorption efficiency of the adsorbent (%), C_e is the concentration of desorbed CDNB in solution (mg L^{-1}); V is the volume of desorption solution (L); m is the dry weight of loaded adsorbent (g); η is the regeneration efficiency of the adsorbent (%); q_i and q_b are the adsorption quantity of regenerative APC and APC in the same experimental conditions, respectively.

3. Results and discussion

3.1. Characterization of PyC and APC

The structural heterogeneity of activated carbon plays an important role in adsorption processes, and numerous methods have consequently been developed and applied for the characterization of this property. In this study, nitrogen adsorption, scanning electron microscopy and XRD methods were used to characterize our carbon samples. Surface chemistry of the carbons was analyzed by FTIR, measurement of acidic and basic functional groups.

3.1.1. Nitrogen adsorption/desorption

Identifying pore structure of adsorbents by the adsorption of inert gases is essential before liquid sorption experiments. Fig. 2(a) illustrates adsorption/desorption isotherms of N_2 at 77 K on PyC and APC. The Brunauer–Emmett–Teller (BET; the most usual standard procedure) was used to find the BET surface area and they are 0.52 and 683 m^2 g^{-1} for PyC and APC, respectively. The result showed that the surface area of PyC was significantly increased after activation.

The structural heterogeneity of porous material was generally characterized in terms of the pore size distribution. Fig. 2(b) shows pore size distribution of PyC and APC. It was seen from Fig. 2(b) that the majority of micropores was created for APC and this supported the result that APC obtained had well-developed microporosity. This figure confirmed that PyC was non-porous materials, while APC was mainly micropores and some mesopores. The average radius of pore was 29.8 and 1.5 nm for PyC and APC, respectively.

3.1.2. Comparison of the external surfaces of PyC and APC using SEM

SEM imaging was used to observe the surface morphology. Figs. 3(a) and (b) show the surface morphology of PyC and APC. This figure showed the differences of the external surfaces of PyC and APC. It was obvious that PyC was non-porous carbons, while APC had cavities on their external surface. It seemed that the cavities on the surfaces of APC resulted from the evaporation of the activating agent (phosphoric acid) in this case during carbonization, leaving the space previously occupied by the activating agent. It is seen from Fig. 3 that there was smooth texture with heterogeneous surface for PyC, while there was rough texture with heterogeneous surface and a variety of randomly distributed pore size for APC. Furthermore, it contained an irregular and highly porous surface, indicating relatively high surface area. This observation can be supported by BET surface area.

3.1.3. X-ray diffraction

Materials can be crystallographically characterized by means of XRD. The XRD curves were shown in Fig. 4. Compared with APC and PyC, there was similar XRD. For these carbons, the diffraction profiles exhibited broad peaks at around 24° which are assigned to the reflection from (002) plane. The occurrence of broad peaks at these 2θ indicates an increasing regularity of crystal structure and resulting in better layer alignment.

3.1.4. FTIR of PyC and APC

FTIR of PyC and APC is shown in Fig. 5. Both spectra showed similar absorption. The presence of broadband around 3,440 cm^{-1} was ascribed to both free and H-bonded –OH stretching vibrations due to alcoholic or phenolic functions, while peak around 2,924 cm^{-1} was assigned to the C–H symmetric and asymmetric vibration mode of methyl and methylene groups. A middle strong band at 1,590–1,640 cm^{-1} can be ascribed to C=C aromatic ring stretching vibration enhanced by polar functional groups. Peak near 1,112 cm^{-1} was corresponding to C–O stretching in acids, alcohols, phenols and ethers [11]. At low wave number district, the small shoulder peak at 865 cm^{-1} is ascribable to C–H out-of-plane

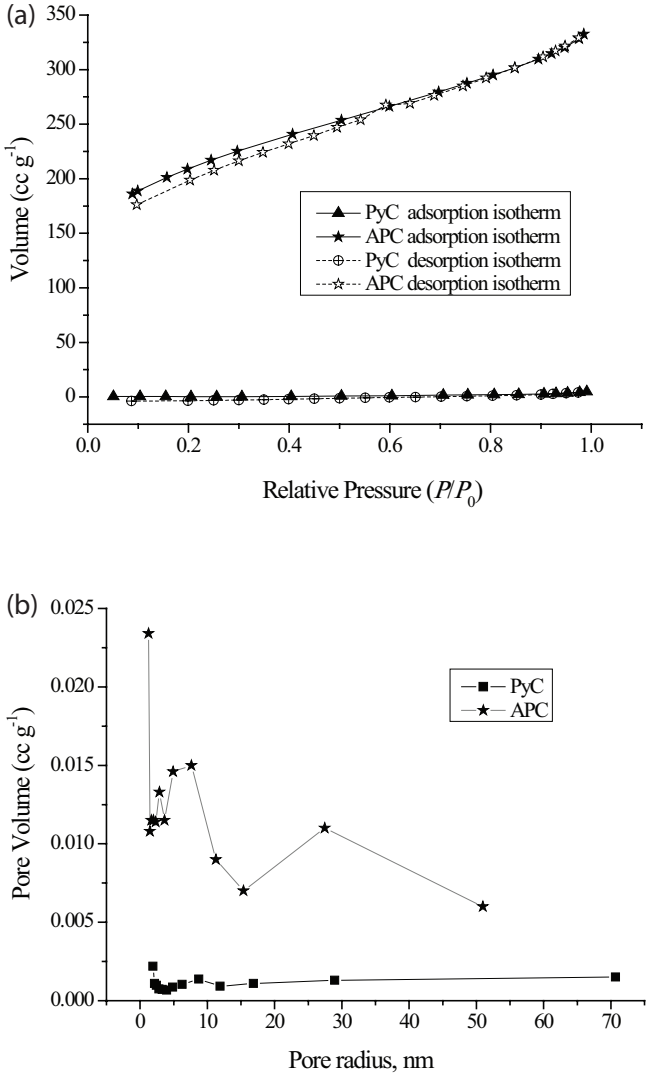

Fig. 2. (a) N_2 adsorption and desorption isotherms for PyC and APC. (b) Pore size distribution of PyC and APC.

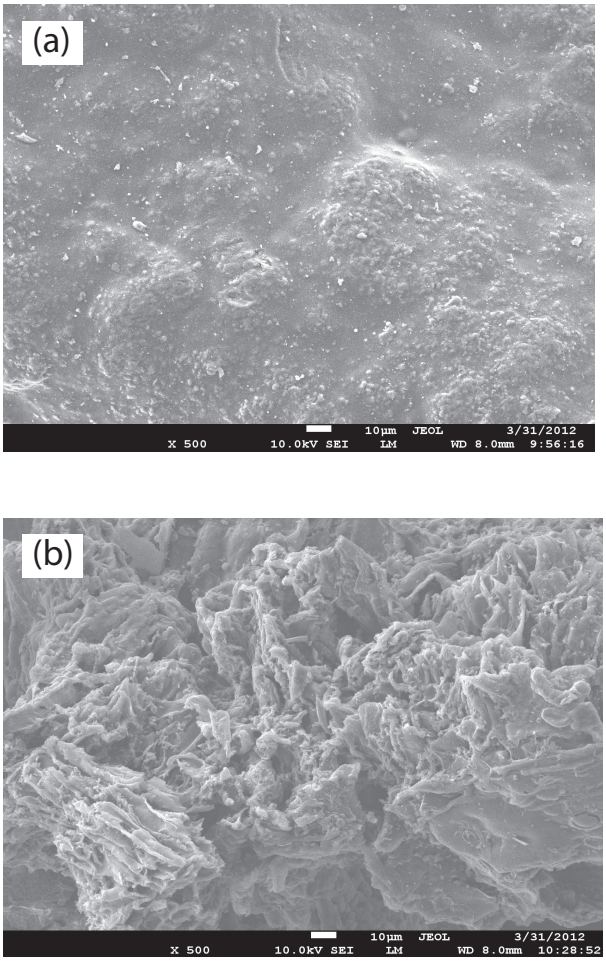

Fig. 3. SEM of PyC (a) and APC (b).

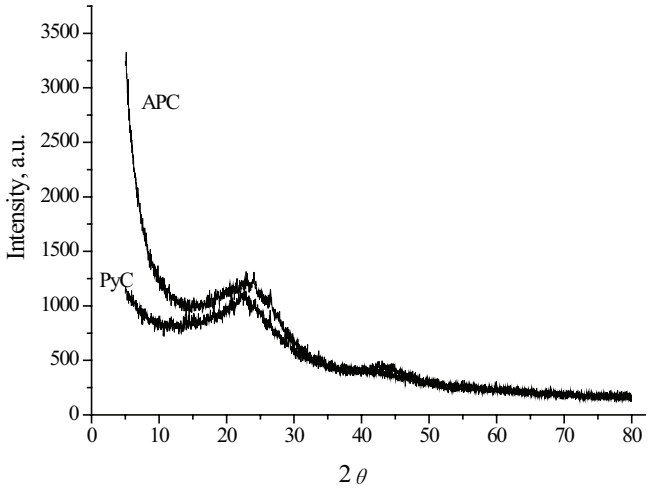

Fig. 4. XRD pattern of PyC and APC.

bending absorption in aromatic ring and C–C stretching is located at 580 and 455 cm^{-1}.

Compared with PyC, the presence of COO– groups in APC was consistent with the peak at approximately 1,558 cm^{-1} which was typically attributed to anti-symmetric stretching vibration. The peak near 1,120 cm^{-1} became slightly strong and this was due to ionized linkage P^{+}–O^{-} in acid phosphate esters and to symmetrical vibration in a chain of P–O–P. Overall, the FTIR results demonstrated qualitative differences in the surface functional groups of PyC and APC.

3.1.5. pH_{pzc} of PyC and APC

The pH of the point of zero charge (pH_{pzc}) of materials depends on the chemical and electronic properties of the functional groups on its surface. The results for the determination of pH_{pzc} are shown in Fig. 6. From Fig. 6, the pH_{pzc} values are approximately 6.7 for PyC and 5.5 for APC, respectively. Therefore, there was a negatively charged surface of adsorbent at pH over this value while there was a positively charged surface of adsorbent at pH below this value.

3.1.6. Elemental analysis and acidic and basic functional groups

The contents of elemental analysis were C 66.4%, H 3.54%, N 0.078% for PyC and C 63.9%, H 2.90%, N 0.011% for APC. The elemental analysis (data not presented) showed that the content of C, N and H decreased with small extent after activation. X-ray fluorescence analysis showed that there were higher content of phosphorus element and lower content of calcium and potassium for APC. But for PyC, phosphorus was not detected and contents of calcium and potassium were higher. The difference was from activation by phosphoric acid and elution by HCl solution. The amount of acidic and basic functional groups of PyC and APC are listed in Table 1. There were more acidic groups and less basic groups for APC and this suggested that activation facilitated the creation of acidity on the surface of PyC. Furthermore, there were more carboxyl group and phenolic group and less lactonic group for APC. The result was consistent with lower pH_{pzc} values of APC. The type and concentration of surface functional groups can play an important role in the adsorption capacity and the removal mechanism of the adsorbates.

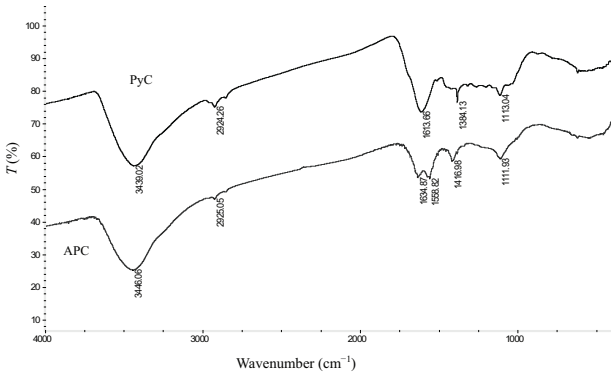

Fig. 5. FTIR of PyC and APC.

3.2. Adsorption study

3.2.1. Effect of solution pH on adsorption quantity

The aqueous solution pH has been reported to present a significant influence on the adsorptive uptake of adsorbate as it impacts on both the surface binding sites of the adsorbent and the ionization process of the adsorbate molecule. In the present study, the effect of pH was investigated between 2 and 10 and the results are displayed in Fig. 7.

It was seen that the solution pH affected adsorption quantity (q_e). The values of q_e changed little in the range pH value of 2.0–5.0 and adsorption quantity was to 122 mg g^{-1}. As pH_{pzc} of APC was 5.5, there was positive charge on surface of APC at pH 2.0–5.0. $–NO_2$ with benzene ring was electron withdrawing group and there was some negative property.

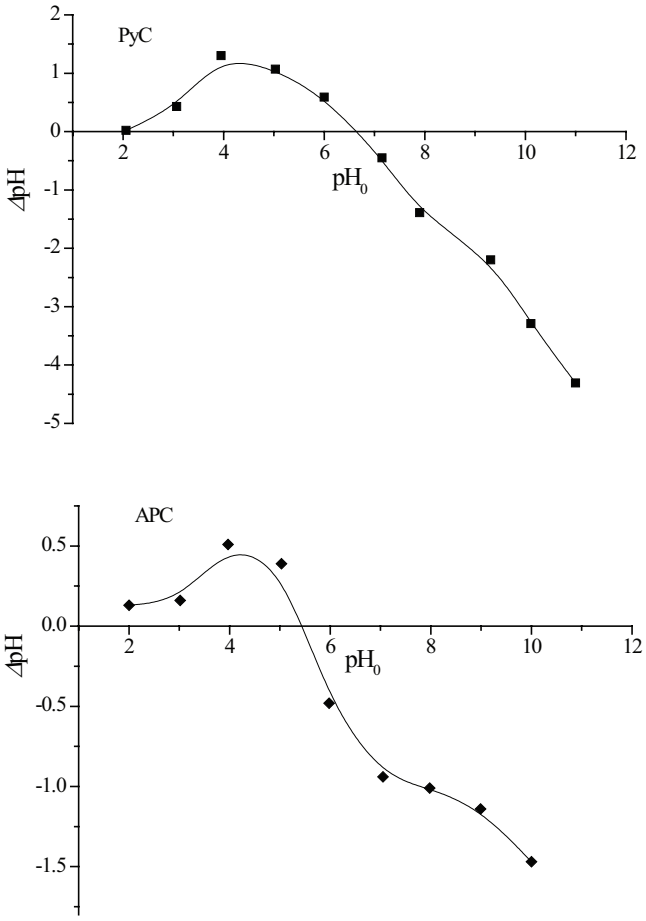

Fig. 6. Determination of pH_{pzc} using pH drift method.

Table 1
Quantity of surface acidic and basic functional groups of PyC and APC

	Surface basicity (mmol g^{-1})	Surface acidity (mmol g^{-1})	Carboxyl (mmol g^{-1})	Lactonic (mmol g^{-1})	Phenolic (mmol g^{-1})
PyC	1.22	1.13	0.608	0.282	0.235
APC	0.167	1.787	1.13	0.189	0.469

So there was some electrostatic attraction between APC and CNDB. When the value of pH was from 5 to 11, the adsorption quantity decreased with some extent. This showed that it was not in favor of adsorption at basic condition as the acidic group onto surface of adsorbent was dissociated and existed in anionic form which decreased the action between CDNB and adsorbent. So the pH of the working solution was adjusted to 4. As CDNB molecule existed as neutral form, and the removal of CDNB was still efficient at basic condition, this suggested that π–π dispersion interactions between adsorbent and adsorbate be dominant in adsorption process.

Compared with APC, there was lower adsorption capacity of CDNB onto PyC (8.45 mg g^{-1}) at the same condition. So compared with PyC, adsorption quantity of APC toward CDNB was 14 times. The significant difference of adsorption quantity was due to the property of adsorbent surface. There was higher surface area and lower pore size, rough surface, more carboxyl group and phenolic group on surface of APC, which was favored of CDNB adsorption. This was also concluded that adsorption capacity of PyC be significantly enhanced after activation.

3.2.2. Effect of NaCl concentration on adsorption quantity

The wastewater containing pollutants has commonly higher salt concentration, and the effects of ionic strength are of some importance in the study of adsorbates onto adsorbents. Fig. 8 shows the effect of NaCl concentration on the values of q_e. From Fig. 8, it is seen that values of q_e changed little with the increase of NaCl concentration. The reason was due to CDNB existed in neutral form and there was little effect with change of ionic strength. This result implied that APC can be used to remove CDNB from practical effluents containing common salts.

3.2.3. Effect of contact time on adsorption quantity

The results of adsorption quantity per gram APC (q_t) at different contact time (t) are shown in Fig. 9.

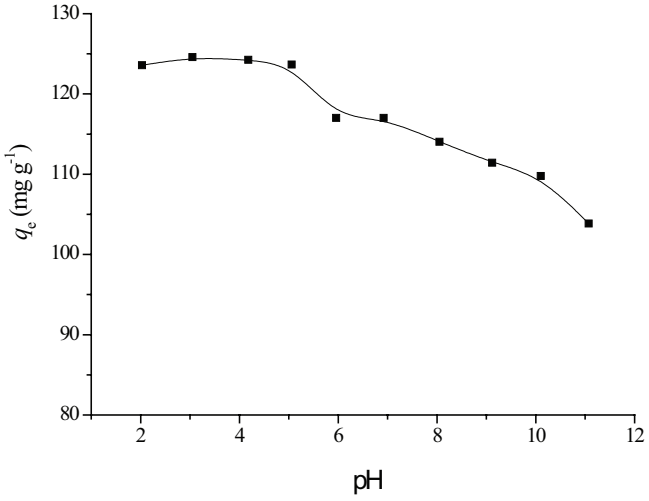

Fig. 7. The effect of solution pH on adsorption quantity (C_0 = 30 mg L^{-1}, dose = 0.2 g L^{-1}, T = 297 K).

From Fig. 9, a three-stage kinetic behavior is evident: a rapid initial adsorption over 60 min, followed by a longer period of much slower uptake 180 min and gradual equilibrium time. The first phase was the instantaneous adsorption stage or external surface adsorption. The second and third phase was the gradual adsorption stage and finally CDNB uptake reached equilibrium. The adsorption quantity was up to 125.2 mg g^{-1}.

In order to predict adsorption kinetic process, the pseudo-first-order kinetic model and the pseudo-second-order kinetic model were used to analyze the experimental data.

The pseudo-first-order kinetic model was generally given as [27]:

$$q_t = q_e(1 - e^{-k_1 t}) \tag{4}$$

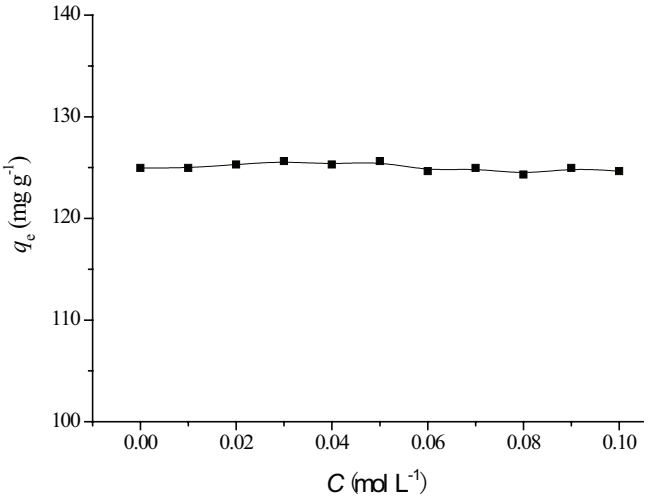

Fig. 8. Effect of NaCl concentration on adsorption quantity (C_0 = 30 mg L^{-1}, dose = 0.2 g L^{-1}, T = 297 K, pH = 4).

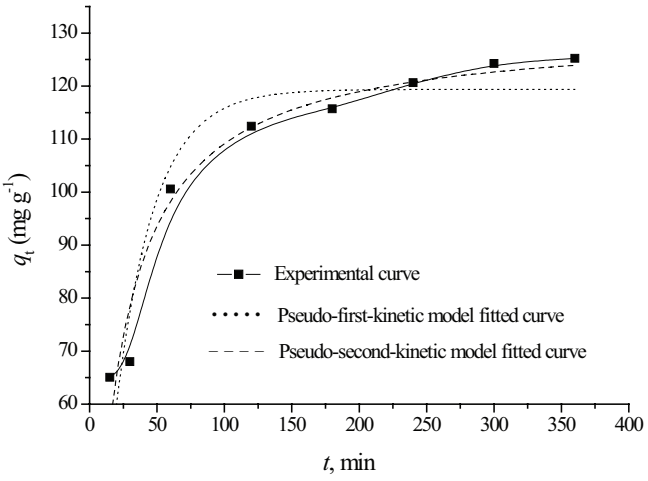

Fig. 9. Effect of contact time on adsorption quantity and fitted curves by kinetic models (C_0 = 30 mg L^{-1}, dose = 0.2 g L^{-1}, T = 297 K, pH = 4).

The pseudo-second-order kinetic model was represented as the following [27]:

$$q_t = \frac{k_2 q_e^2 t}{1 + k_2 q_e t} \quad (5)$$

where q_e and q_t (mg·g^{-1}) were the amounts of CDNB adsorbed on adsorbent at equilibrium and at any time t, respectively. And k_1 was the rate constant of pseudo-first-order kinetic model (min^{-1}). And k_2 was the rate constant of pseudo-second-order kinetic model (g·mg^{-1}·min^{-1}).

The kinetic parameters can be calculated from non-linear regressive analysis using software Origin 7.5. The parameters of two models, together with determined coefficient (R^2) and average relative error (x^2) are listed in Table 1. Furthermore, the comparison between experimental curves and fitted curves are also illustrated in Fig. 8.

As shown in Table 2, there were lower value of R^2 and higher value of x^2 about pseudo-first-order kinetic model and this showed that this model was not appropriate to fit the kinetic process. But for pseudo-second-order kinetic model, there were higher value of R^2 and lower value of x^2. Value of q_e in Table 1 (130.8 mg g^{-1}) was very close to value of q_e from experiment. Furthermore, the fitted curve from pseudo-second-order kinetic model was also closer to experimental curve. So pseudo-second-order kinetic model could describe the adsorption kinetics and the rate determining step could be chemical adsorption in this adsorption process [27]. This implied that valency forces may be involved during this process by exchange or sharing electrons between APC and CDNB.

In order to assess the nature of the diffusion process responsible for the adsorption of CDNB on APC, attempts were made to calculate the coefficients of the process as explained by Chabani et al. [28]. Assuming spherical geometry for APC, the overall rate constant of the process can be correlated with the pore diffusion coefficient (D_p) and the film diffusion coefficient (D_f) independently according to reference [27,29,30] as described below:

$$t_{1/2} = \frac{1}{k_2 q_e} \quad (6)$$

$$t_{1/2} = \frac{0.03 r^2}{D_p} \quad (7)$$

$$D_p = \frac{0.03 r^2}{t_{1/2}} \quad (8)$$

$$D_f = \frac{0.23 r \varepsilon}{t_{1/2}} \times \frac{q_e}{C_0} \quad (9)$$

where r (0.0149–0.0125 cm) is the radius of the adsorbent, ε is the film thickness (10^{-3} cm) and $t_{1/2}$ is the time for half sorption (min).

Values of $t_{1/2}$ and D_p calculated according to Eqs. (6) and (8) were 19.72 min and 3.96 × 10^{-9} to 5.33 × 10^{-9} cm^2 s^{-1}, respectively. The pore diffusion rate constants were in the order of 10^{-10} to 10^{-11} cm^2·s^{-1} and values of D_p in this system was over one order, suggesting that the pore diffusion in this adsorption process was not significant.

Values of D_f calculated according to Eq. (9) were from 1.06 × 10^{-8} to 1.26 × 10^{-8} cm^2 s^{-1}. The value of the film diffusion coefficient (D_f) should be in the range 10^{-6} to 10^{-8} cm^2 s^{-1} and values of D_f was in this range. So it clearly appeared that CDNB removal on APC was controlled by film diffusion process.

3.2.4. The effect of equilibrium CDNB concentration on adsorption quantity

The effect of the equilibrium concentration of CDNB in the solutions on adsorption is shown in Fig. 10 (adsorption isotherm). As seen from Fig. 10, equilibrium uptake increased with the increasing of CDNB concentrations at the range of experimental concentration. This was a result of the increase in the driving force the concentration gradient. It was also found that there was highest adsorption quantity at 303 K. At experimental conditions, adsorption quantity was improved with the increase of temperature below 303 K, while it was decreased when temperature was over 303 K. In another words, the adsorption process was endothermic as temperature was below 303 K while the process was exothermic as temperature was over 303 K.

The equilibrium isotherm is significant to design and optimize the adsorption system for the removal of adsorbate from wastewater. Both common adsorption isotherm equilibrium models, Langmuir model and Freundlich model, were used for the analysis of the APC–CDNB adsorption system. Two models are expressed in the following.

Langmuir isotherm model [31]:

$$q_e = \frac{q_m K_L c_e}{1 + K_L c_e} \quad (10)$$

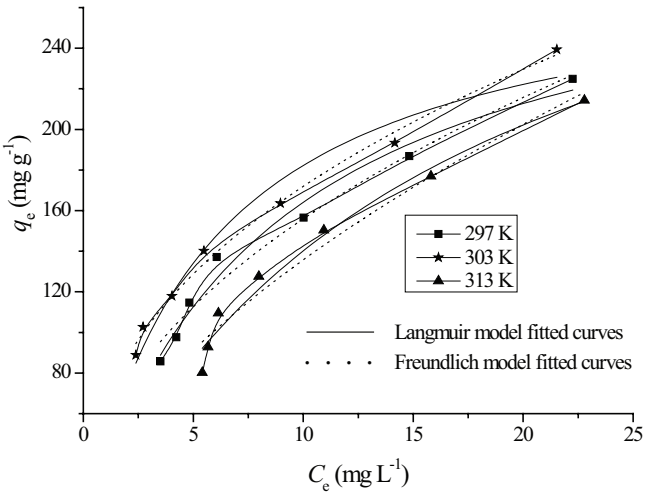

Fig. 10. Adsorption isotherms and fitted curves at various temperatures (pH = 4).

Table 2
Parameters of adsorption models by non-linear regressive analysis

Models	Parameters			
Langmuir model	K_L (L mg^{-1})	q_m (mg g^{-1})	R^2	x^2
297 K	0.119 ± 0.015	302.3 ± 17.6	0.981	56.1
303 K	0.178 ± 0.028	284.5 ± 17.9	0.968	107.8
313 K	0.0630 ± 0.010	362.8 ± 33.0	0.979	56.6
Freundlich model	K_F	$1/n$	R^2	x^2
297 K	53.02 ± 4.36	0.468 ± 0.033	0.977	69.3
303 K	65.81 ± 2.57	0.417 ± 0.016	0.993	23.3
313 K	36.01 ± 4.43	0.576 ± 0.047	0.968	88.8
Pseudo-first-order kinetic model	q_e (mg g^{-1})	k_1 (min^{-1})	R^2	x^2
	119.4 ± 4.0	0.0351 ± 0.0055	0.886	78.9
Pseudo-second-order kinetic model	q_e (mg g^{-1})	k_2 (g mg^{-1} min^{-1})	R^2	x^2
	130.8 ± 3.8	0.00039 ± 0.00007	0.951	34.2

Note: $x^2 = \sum\left(q - q_c\right)^2$, q and q_c are the experimental value and calculated value according to the model, respectively.

Freundlich isotherm model [32]:

$$q_e = K_F c_e^{1/n} \tag{11}$$

where K_L and q_m are constants related to affinity of the binding sites (L mg^{-1}) and adsorption capacity (mg g^{-1}), respectively; $1/n$ and K_F are the Freundlich constants related to adsorption intensity of the adsorbent and the adsorption capacity, respectively.

The parameters of two models and determined coefficients were also listed in Table 2 and the fitted curves are shown in Fig. 10.

It is observed from Table 2 that there were higher values of R^2 and lower values of x^2 for both model, this implied that both models can be applied to fit the adsorption equilibrium process. But the value of q_m from Langmuir model was lowest at 303 K, this was opposite to experimental results. This showed that Langmuir model was not available to fit the data at 303 K. Furthermore, fitted curves from Freundlich model were more close to experimental curves (seen in Fig. 10). So Freundlich model was better to predict the equilibrium process. This result suggested that the CDNB adsorption be heterogeneous and adsorption energy exponentially decrease on completion of the adsorption centers of an adsorbent.

The value of q_m from Langmuir model was up to 302.3 ± 17.6 mg g^{-1} at 297 K. It was also found that parameter of n was within 1–10 and this indicated that CDNB ions were favorably adsorbed by APC at all the temperatures studied [33,34].

3.3. Regeneration of exhausted APC

Regeneration of saturated adsorbent was crucial to evaluate the reusability of the adsorbents and to elucidate the mechanism of adsorption [35–38]. If CDNB adsorbed on surface of APC was desorbed easily by deionized water, the attachment of CDNB onto APC was of feeble binding force. The chemisorption would be verified if high desorption efficiency was obtained using organic solution, such as ethanol. In this work, two different desorption solutions were tested in batch system to find optimal reagent. And regeneration efficiency (p) was found to be 8.2%, 60.2% for deionized water and 70% ethanol, respectively. Thus, it was rational to refer that the action between CDNB and APC be controlled predominantly by chemisorption. The regenerated APC was repeatedly used to adsorb CDNB when 70% ethanol served as elution solution. The desorption efficiency was 99.0%, 81.6% and 71.9% while regeneration efficiency (η) was 60.2%, 37.7% and 19.1% during three adsorption–desorption cycles. This showed that adsorption quantity significantly decreased after regeneration.

4. Conclusion

APC was prepared through activation of pine-sawdust pyrolytic char (PyC) by phosphoric acid impregnation and microwave. Surface area of APC was significantly increased while there were more acidic groups and less basic groups for APC. CDNB was as adsorbate to study the adsorption property of APC. There was higher adsorption capacity and the adsorption quantity from experiment was up to 220.8 mg g^{-1} at 297 K. Langmuir model and Freundlich model can predict the equilibrium process while pseudo-second-order kinetic model can fit kinetic data and it was controlled by film diffusion process. Exhausted APC can be regenerated by 70% ethanol. It was promising that APC can be used as good adsorbent to remove CDNB from solution.

Acknowledgments

This work was financially supported by the Henan province basis and advancing technology research project (142300410224) and Educational Department of Henan Province (13A150650).

References

[1] L.S. Zhang, Treatment Technique of Printing and Dyeing Wastewater and Typical Engineering, Chemical Industry Press, Beijing, 2005 (in Chinese).

[2] Z. Aksu, Application of biosorption for the removal of organic pollutants: a review, Process Biochem., 40 (2005) 997–1026.

[3] I. Ali, M. Asim, T.A. Khan, Low cost adsorbents for the removal of organic pollutants from wastewater, J. Environ. Manage., 113 (2012) 170–183.

[4] X. Xu, B.Y. Gao, B. Jin, Q.Y. Yue, Removal of anionic pollutants from liquids by biomass materials: a review, J. Mol. Liq., 215 (2016) 565–595.

[5] W.H. Zou, P. Han, Y.L. Lia, X. Liu, X.T. He, R.P. Han, Equilibrium, kinetic and mechanism study for the adsorption of neutral red onto rice husk, Desal. Wat. Treat., 12 (2009) 210–218.

[6] W.S. Wan Ngah, M.A.K.M. Hanafiah, Removal of heavy metal ions from wastewater by chemically modified plant wastes as adsorbents: a review, Bioresour. Technol., 99 (2008) 3935–3948.

[7] O. Ioannidou, A. Zabaniotou, Agricultural residues as precursors for activated carbon production—a review, Renew. Sustain. Energy Rev., 11 (2007) 1966–2005.

[8] D. Mohan, C.U. Pittman Jr., P.H. Steele, Pyrolysis of wood/biomass for bio-oil: a critical review, *Energy Fuels, 20* (2006) 848–889.

[9] J.W. Lee, M. Kidder, B.R. Evans, S. Paik, A.C. Buchanan III, C.T. Garten, R.C. Brown, Characterization of biochars produced from corn stovers for soil amendment, Environ. Sci. Technol., 44 (2010) 7970–7974.

[10] J. Komkiene, E. Baltrenaite, Biochar as adsorbent for removal of heavy metal ions [cadmium(II), copper(II), lead(II), zinc(II)] from aqueous phase, Int. J. Environ. Sci. Technol., 13 (2016) 471–482.

[11] Y.L. Liu, X.R. Zhao, J.L. Li, D. Ma, R.P. Han, Characterization of bio-char from pyrolysis of wheat straw and its evaluation on methylene blue adsorption, Desal. Wat. Treat., 46 (2012) 115–123.

[12] X.N. Zhang, G.Y. Mao, Y. Shang, X.F. Ren, R.P. Han, Adsorption of anionic dye on magnesium hydroxide coated pyrolytic biochar and reuse by microwave irradiation, Int. J. Environ. Sci. Technol., 11 (2014) 1439–1448.

[13] F.K. Yuen, B.H. Hameed, Recent developments in the preparation and regeneration of activated carbons by microwaves, Adv. Colloid Interface Sci., 149 (2009) 19–27.

[14] D.A. Jones, T.P. Lelyveld, S.D. Mavrofidis, S.W. Kingman, N.J. Miles, Microwave heating applications in environmental engineering—a review, Resour. Conserv. Recycl., 34 (2002) 75–90.

[15] Md A. Hossain, J. Jewaratnam, P. Ganesan, J.N. Sahu, S. Ramesh, S.C. Poh, Microwave pyrolysis of oil palm fiber (OPF) for hydrogen production: parametric investigation, Energy Convers. Manage., 115 (2016) 232–243.

[16] R.H. Hesas, A. Arami-Niya, W.M.A.W. Daud, J.N. Sahu, Comparison of oil palm shell-based activated carbons produced by microwave and conventional heating methods using zinc chloride activation, J. Anal. Appl. Pyrolysis, 104 (2013) 176–184.

[17] K.R. Thines, E.C. Abdullah, N.M. Mubarak, M. Ruthiraan, Synthesis of magnetic biochar from agricultural waste biomass to enhancing route for waste water and polymer application: a review, Renew. Sustain. Energy Rev., 67 (2017) 257–276.

[18] H. Deng, L. Yang, G.H. Tao, J.L. Dai, Preparation and characterization of activated carbon from cotton stalk by microwave assisted chemical activation—application in methylene blue adsorption from aqueous solution, J. Hazard. Mater., 166 (2009) 1514–1521.

[19] K.Y. Foo, B.H. Hameed, Mesoporous activated carbon from wood sawdust by K_2CO_3 activation using microwave heating, Bioresour. Technol., 111 (2012) 425–432.

[20] W. Xiao, R.D. Zhang, Y.B. Song, R.P. Han, Y.Q. Li, Adsorption of 4-chloro-2,5-dimethoxy nitrobenzene by activated pyrolytic char from pine sawdust, Adv. Mater. Res., 884–885 (2014) 190–194.

[21] M.J. Ahmed, Application of agricultural based activated carbons by microwave and conventional activations for basic dye adsorption: review, J. Environ. Chem. Eng., 4 (2016) 89–99.

[22] A. Demirbas, Agricultural based activated carbons for the removal of dyes from aqueous solutions: a review, J. Hazard. Mater., 167 (2009) 1–9.

[23] R.H. Hesas, W.M.A.W. Daud, J.N. Sahu, A. Arami-Niya, The effects of a microwave heating method on the production of activated carbon from agricultural waste: a review, J. Anal. Appl. Pyrolysis, 100 (2013) 1–11.

[24] O. Ioannidou, A. Zabaniotou, Agricultural residues as precursors for activated carbon production—a review, Renew. Sustain. Energy Rev., 11 (2007) 1966–2005.

[25] C.S. Zhang, L. Yang, Y.G. Liu, Q.L. Yang, R.Q. Zhang, Study on biomass pyrolysis in a fluidized-bed reactor, Renew. Energy Res., 25 (2007) 29–33 (in Chinese).

[26] H.P. Boehm, Some aspects of the surface chemistry of carbon blacks and other carbons, Carbon, 32 (1994) 759–769.

[27] Y.S. Ho, J.C.Y. Ng, G. McKay, Kinetics of pollutant sorption by biosorbents: review, Sep. Purif. Methods, 29 (2000) 189–232.

[28] M. Chabani, A. Amraneb, A. Bensmaili, Kinetic modeling of the adsorption of nitrates by ion exchange resin, Chem. Eng. J., 125 (2006) 111–117.

[29] S.V. Mohan, S.V. Ramanaiah, P.N. Sharma, Biosorption of direct azo dye from aqueous phase onto *Spirogyra* sp I02: evaluation of kinetics and mechanistic aspects, Biochem. Eng. J., 38 (2008) 61–69.

[30] W.J. Weber, J.C. Morris, Advances in Water Pollution Research: Removal of Biologically-Resistant Pollutants from Waste Waters by Adsorption, Proc. International Conference on Water Pollution Symposium, Vol. 2, Pergamon Press, Oxford, 1962, pp. 231–266.

[31] I. Langmuir, The constitution and fundamental properties of solids and liquids, J. Am. Chem. Soc., 38 (1916) 2221–2295.

[32] H.M.F. Freundlich, Uber die adsorption in lasungen, Z. Phys. Chem., 57 (1906) 385–470.

[33] Z. Aksu, Determination of the equilibrium, kinetic and thermodynamic parameters of the batch biosorption of nickel(II) ions onto *Chlorella vulgaris*, Process Biochem., 38 (2002) 89–99.

[34] R.P. Han, J.J. Zhang, P. Han, Y.F. Wang, Z.H. Zhao, M.S. Tang, Study of equilibrium, kinetic and thermodynamic parameters about methylene blue adsorption onto natural zeolite, Chem. Eng. J., 145 (2009) 496–504.

[35] S. Sadaf, H.N. Bhatti, Evaluation of peanut husk as a novel, low cost biosorbent for the removal of Indosol Orange RSN dye from aqueous solutions: batch and fixed bed studies, Clean Technol. Environ. Policy, 16 (2014) 527–544.

[36] R.P. Han, Y. Wang, Q. Sun, L.L. Wang, J.Y. Song, X.T. He, C.C. Dou, Malachite green adsorption onto natural zeolite and reuse by microwave irradiation, J. Hazard. Mater., 175 (2010) 1056–1061.

[37] T. Zhou, W.Z. Lu, L.F. Liu, H.M. Zhu, Y.B. Jiao, S.S. Zhang, R.P. Han, Effective adsorption of light green anionic dye from solution by CPB modified peanut in column mode, J. Mol. Liq., 211 (2015) 909–914.

[38] R.D. Zhang, J.H. Zhang, X.N. Zhang, C.C. Dou, R.P. Han, Adsorption of congo red from aqueous solutions using cationic surfactant modified wheat straw in batch mode: kinetic and equilibrium study, J. Taiwan Inst. Chem. Eng., 45 (2014) 2578–2583.